Parallel multicanonical study of the three-dimensional Blume-Capel model

Zierenberg, J. , Fytas, N. G. and Janke, W.

Original citation:
Zierenberg, J. , Fytas, N. G. and Janke, W. (2015) Parallel multicanonical study of the three-dimensional Blume-Capel model. PHYSICAL REVIEW E, volume 91 (3): 032126

DOI: 10.1103/PhysRevE.91.032126
URL: http://link.aps.org/abstract/PRE/v91/i3/2015/e032126

Publisher: American Physical Society

Parallel multicanonical study of the three-dimensional Blume-Capel model

Johannes Zierenberg,[1] Nikolaos G. Fytas,[2] and Wolfhard Janke[1]
[1]*Institut für Theoretische Physik, Universität Leipzig, Postfach 100 920, D-04009 Leipzig, Germany*
[2]*Applied Mathematics Research Centre, Coventry University, Coventry CV1 5FB, United Kingdom*
(Received 15 December 2014; published 18 March 2015)

We study the thermodynamic properties of the three-dimensional Blume-Capel model on the simple cubic lattice by means of computer simulations. In particular, we implement a parallelized variant of the multicanonical approach and perform simulations by keeping a constant temperature and crossing the phase boundary along the crystal-field axis. We obtain numerical data for several temperatures in both the first- and second-order regime of the model. Finite-size scaling analyses provide us with transition points and the dimensional scaling behavior in the numerically demanding first-order regime, as well as a clear verification of the expected Ising universality in the respective second-order regime. Finally, we discuss the scaling behavior in the vicinity of the tricritical point.

DOI: 10.1103/PhysRevE.91.032126 PACS number(s): 05.50.+q, 75.10.Nr, 64.60.Cn, 75.10.Hk

I. INTRODUCTION

The Blume-Capel (BC) model consisting of a spin-1 Ising Hamiltonian with a single-ion uniaxial crystal-field anisotropy [1,2] is one of the most studied models in the communities of statistical mechanics and condensed matter physics. This is not only because of the relative simplicity with which approximate calculations for this model can be carried out and tested, as well as the fundamental theoretical interest arising from the richness of its phase diagram, but also because versions and extensions of the model can be applied for the description of many different physical systems, some of them being multicomponent fluids, ternary alloys, and ^{3}He-^{4}He mixtures [3]. Recent applications of the BC model include analyses of ferrimagnets, as discussed in a thorough contribution by Selke and Oitmaa [4].

The BC model is described by the Hamiltonian

$$\mathcal{H} = -J \sum_{\langle ij \rangle} \sigma_i \sigma_j + \Delta \sum_i \sigma_i^2 = E_J + \Delta E_\Delta, \qquad (1)$$

where the spin variables σ_i take on the values $\{-1,0,+1\}$, $\langle ij \rangle$ indicates summation over all nearest-neighbor pairs of sites, and $J > 0$ is the ferromagnetic exchange interaction (here we set $J = 1$ and $k_B = 1$ to fix the temperature scale). The parameter Δ is known as the crystal-field coupling that controls the density of vacancies ($\sigma_i = 0$). For $\Delta \to -\infty$ vacancies are suppressed and the model maps onto the Ising model. We always employ periodic boundary conditions. Note here that the second formulation of the Hamiltonian (1), via the definitions of E_J and E_Δ, will allow us to define the necessary observables for the application of our finite-size scaling (FSS) scheme that is discussed in detail below.

As is well known, the pure and disordered versions of the model of Eq. (1) have been analyzed, besides the original mean-field theory [1,2], by a variety of approximations and numerical approaches, in both two (2D) and three dimensions (3D). These include the real-space renormalization group [5], Monte Carlo renormalization-group calculations [6], ϵ-expansion renormalization groups [7], high- and low-temperature series expansions [8], a phenomenological FSS analysis using a strip geometry [9,10], and, of course, Monte Carlo simulations [11–22].

The phase diagram of the pure model consists of a segment of continuous Ising-like transitions at high temperatures and low values of the crystal field. This ends at a tricritical point (Δ_t, T_t), where it is joined with a second segment of first-order transitions ending for $T = 0$ at $\Delta_0 = zJ/2$, with z denoting the coordination number of the considered lattice. In the present case of a simple cubic lattice, where $z = 6$, it follows that $\Delta_0 = 3$. A general sketch of the phase diagram is given in Fig. 1 and is outlined in the relevant caption. The location of the tricritical point, marked by the black diamond in Fig. 1, has been estimated by Deserno [14] using a microcanonical Monte Carlo approach to be $(\Delta_t, T_t) = (2.844\,79(30), 1.4182(55))$.

The scope of the present paper is to present a complementary study of the 3D BC model embedded in the simple cubic lattice. Our simulations follow a sophisticated numerical scheme, outlined in Sec. II, using as a platform the multicanonical approach. This is especially suitable for the study of systems that undergo a first-order phase transition, where it is well known that numerical simulation is a hard task to perform. One interesting aspect of the present work is that we cross, in our simulations, the phase boundary of the system along the crystal-field axis, keeping the temperature fixed. Thus, we obtain relevant thermodynamic observables as a function of the crystal field Δ and we perform a FSS analysis on a different basis. This analysis is presented in Sec. III, in both the first- and second-order regimes of the model, where the second-order regime is used as a test case of our scheme and more attention is paid to the first-order regime of the phase diagram, which is computationally much more challenging. In particular, we consider three different temperatures: one in the second-order regime, $T_1 = 2.0$, and two in the first-order regime, $T_2 = 1.0$ and $T_3 = 0.9$. Moreover, we discuss the scaling properties in the vicinity of the proposed tricritical point by performing additional simulations and relevant analyses at the temperature $T_t = 1.4182$ suggested in Ref. [14]. This contribution is ended in Sec. IV, where a brief summary of our conclusions is given together with an outlook for future work.

II. NUMERICAL METHOD AND SCALING OBSERVABLES

We apply the multicanonical method [23,24] with the slight modification to yield a flat histogram not in the total energy E, but rather in E_Δ. The multicanonical method allows

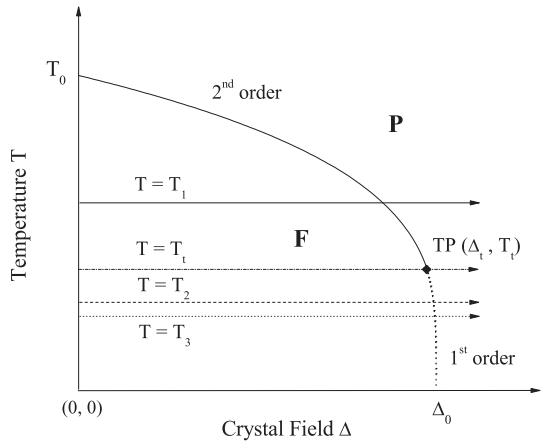

FIG. 1. General sketch of the phase diagram of the 3D BC model in the temperature–crystal-field plane. The phase boundary separates the ferromagnetic (**F**) phase from the paramagnetic (**P**) phase, in which the solid line indicates continuous phase transitions and the dotted line first-order phase transitions. The two lines merge at the tricritical point (TP), as highlighted by the black diamond. The limiting cases of $T = 0$ and $\Delta = 0$ are marked on the relevant axis with $\Delta_0 = 3$ and $T_0 = 3.195(1)$ [22], respectively. The horizontal arrows illustrate the direction of crossing the phase boundary at fixed temperatures, studied in this work, in both the second-order ($T_1 = 2.0$) and the first-order ($T_2 = 1.0$ and $T_3 = 0.9$) regimes, as well as in the vicinity of the tricritical point ($T_t = 1.4182$) [14].

one to increase the probability to sample otherwise suppressed states and, with it, overcome emerging barriers. Hence, it is an optimal tool to study first-order phase transitions. The canonical expectation value weights all observables of the phase space with the Boltzmann weight, which leads to the general form

$$\langle O \rangle = \frac{1}{Z} \sum_x O(x) e^{-\beta E(x)}, \tag{2}$$

where $Z = \sum_x e^{-\beta E(x)}$ is the partition sum, $\beta = 1/T$ is the inverse temperature, and x stands for the spin configurations.

For the usual multicanonical method, the Boltzmann weight in the canonical probability distribution $\exp\{-\beta E(x)\}$ is replaced by a weight function $W[E(x)]$ that is iteratively modified to yield a flat energy histogram. At this point, we can rewrite $E = E_J + \Delta E_\Delta$, separate the probability distribution, and replace the Boltzmann weight depending on E_Δ:

$$e^{-\beta E_J} e^{-\beta \Delta E_\Delta} \to e^{-\beta E_J} W(E_\Delta). \tag{3}$$

Considering a fixed inverse temperature β, one is then able to iteratively adapt $W(E_\Delta)$ in order to yield a flat histogram in E_Δ. This is, in fact, quite similar to multimagnetic simulations and also suited for the application of a parallel implementation of the multicanonical method [25]. We made use of this parallelization with up to 36 cores, which speeds up the iteration process and provides 36 independent production runs. The canonical expectation values at a certain point (Δ, T) may then be estimated with standard histogram and time-series reweighting techniques [26]. Since the multicanonical simulation is still an importance sampling Markov chain, one only needs to consider the multicanonical variable E_Δ, illustrated for the case of time-series reweighting of a given observable O:

$$\langle O \rangle_{\beta,\Delta} = \frac{\sum_x O(x) e^{-\beta \Delta E_\Delta(x)} W^{-1}[E_\Delta(x)]}{\sum_x e^{-\beta \Delta E_\Delta(x)} W^{-1}[E_\Delta(x)]}. \tag{4}$$

Here $\langle \cdots \rangle$ clearly refers to the estimator of the expectation value and we drop the subscripts in the following. Figure 2 shows an example of the reweighted probability distributions of $e_\Delta = E_\Delta/V$, where $V = L^3$ and L denotes the linear system size, at the transition field Δ_{eqh}, i.e., where the distribution shows two peaks of equal height. Well inside the first-order regime the system shows a barrier increasing with the system size, characteristic of the nature of the transition, which reaches at $T_3 = 0.9$ already for a system size of $V = 24^3$ spins the order of 10^{-130}; see Fig. 2(a). On the other hand, at the proposed tricritical point (see panel (b) with numerical data obtained at $T_t = 1.4182$ [14]) no definite judgement can be made. We observe that the distributions still show a double-peaked structure, yet with a much smaller barrier,

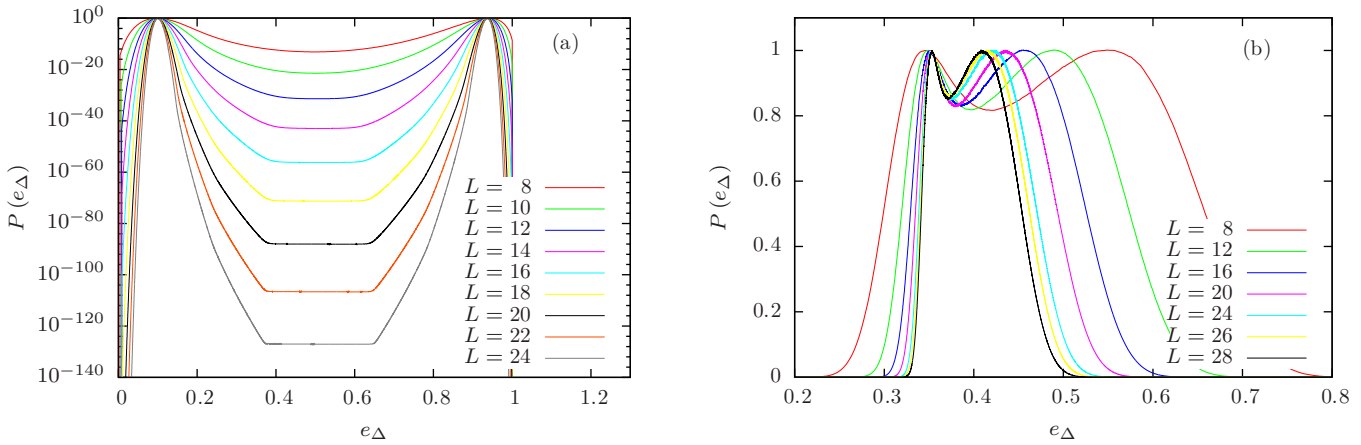

FIG. 2. (Color online) Illustration of the reweighted probability distribution at the transition field Δ_{eqh} with respect to $e_\Delta = E_\Delta/V$ at (a) $T = 0.9$, which is well inside the first-order regime of the system (note the strongly increasing barrier with the system size), exhibiting a major suppression of intermediate states which is common for first-order transitions, and at (b) $T = T_t = 1.4182$, which is in the vicinity of the tricritical point.

which does not diverge with increasing system size. A more illuminating discussion of this special temperature is given at the end of Sec. III.

It is worth noting here that the E_Δ are always integer in the range $[0,V]$, which is a major advantage for the application of the present method. This would not be the case for the usual multicanonical [23,24] and Wang-Landau [27] methods at fixed Δ based on the total energy E, because $E \in \mathbb{R}$ for noninteger values of Δ. Additionally, our previous experience with the application of the Wang-Landau method to the BC model in the low-temperature regime for a fixed value of Δ suggested that one needs to be extremely careful in the details of implementation. For instance, the need to simulate large enough system sizes leads to the inevitable application of a multirange approach of the Wang-Landau method, that is, splitting the energy range in many subintervals [18]. This approach, although appearing to be much faster than the straightforward one-range implementation, may give rise to several problems with respect to the breaking of ergodicity of the process [28–30] and possible distortions (systematic errors) induced on the density of states [31]. On the other hand, the numerical framework developed and applied in the current paper does not suffer from this type of inherent problem. On the contrary, the parallelized variant of the multicanonical approach used, combined with the orthogonal scaling of the phase boundary has proven to be a promising scheme for the first-order transition regime. This will be clearly shown in the following section with the accurate estimation of transition points Δ^* even for temperatures $T < 1$, which is a commonly accepted, harsh numerical task. Still, for the second-order regime both the current approach and any other type of generalized ensemble sampling method would give comparable results within the statistical errors as we have already verified by our preliminary numerical tests. In fact, the modification to a flat-histogram method in a subenergy is not restricted to the present model or a spin system in general and has been applied in a similar way also to a polymer system in disorder [32]. Moreover, the formulation for other generalized ensemble methods is straightforward.

In order to obtain transition points for the FSS analysis, one usually considers the peak of the specific heat C, magnetic susceptibility χ, or any other suitable temperature derivative of an order parameter [26]. In principle, the magnetic properties of the system show a more reliable behavior when one is interested in obtaining accurate estimates of critical points and it is a common practice along these lines to first estimate the magnetic exponents β, γ, and ν, and then, via the hyperscaling relation, the exponent α of the specific heat. However, also other scaling approaches based on a different philosophy have been successfully used in the literature, depending always on the direction of intersecting the phase boundary of the model under study. For instance, it has been shown that for the 3D random-field Ising model at zero temperature, the field derivative of the bond energy E_J defines a specific-heat-like quantity from which one may produce accurate estimates of the critical exponent ratio α/ν and whose shift behavior defines correct critical points in the field-temperature plane [33].

For the present study, where we are crossing the phase diagram at fixed temperature along the crystal-field axis, we may as well consider instead of the standard definitions, the field derivative of the form $\partial/\partial\Delta$. The derivative of the expectation value (2) yields

$$\frac{\partial\langle O\rangle}{\partial\Delta} = -\beta[\langle O E_\Delta\rangle - \langle O\rangle\langle E_\Delta\rangle] + \left\langle \frac{\partial}{\partial\Delta} O \right\rangle, \qquad (5)$$

which is similar to any specific-heat-like quantity because, in general, the observable is independent on the variable and the last term drops out. This is true for either E_i, where $i = J$, or Δ; however, the total energy $E = E_J + \Delta E_\Delta$ is no longer independent on the field, which leads to

$$\begin{aligned}\frac{\partial\langle E\rangle}{\partial\Delta} &= -\beta[\langle E E_\Delta\rangle - \langle E\rangle\langle E_\Delta\rangle] + \langle E_\Delta\rangle \\ &= \frac{\partial\langle E_J\rangle}{\partial\Delta} + \Delta\frac{\partial\langle E_\Delta\rangle}{\partial\Delta} + \langle E_\Delta\rangle. \qquad (6)\end{aligned}$$

However, the last line suggests—expecting a critical or diverging behavior—that we may limit our consideration to either of the energy contributions. In fact, we consider here only the field derivative of the spin-spin interaction term,

$$C(\Delta) = \frac{\partial\langle E_J\rangle}{\partial\Delta} = -\beta[\langle E_J E_\Delta\rangle - \langle E_J\rangle\langle E_\Delta\rangle]. \qquad (7)$$

Similar considerations may apply also for other suitably defined thermodynamic functions that could provide us, for instance, with estimates of magnetic exponents mentioned above. Yet, this task goes beyond the scope of the present work where we focus on the first-order transition regime of the BC model and target only at a qualitative comparison to the expected Ising criticality in the second-order transition regime. In fact, this comparison becomes even more clear via the use of the straightforwardly defined specific-heat-like quantity (7).

Relevant plots of $C(\Delta)$ can be found in the next section in Figs. 3 and 5 and are discussed there. However, it is obvious from these illustrations that there exists clearly a maximum of $C(\Delta)$ that moreover shows a shift behavior as well. Let us define now Δ_L^* as the crystal-field value at which $C(\Delta)$ attains its maximum, and as we shall see below this defines a suitable pseudocritical, or pseudotransition, parameter that carries in itself the approach to the thermodynamic limit in the second- and first-order regime of the model, respectively.

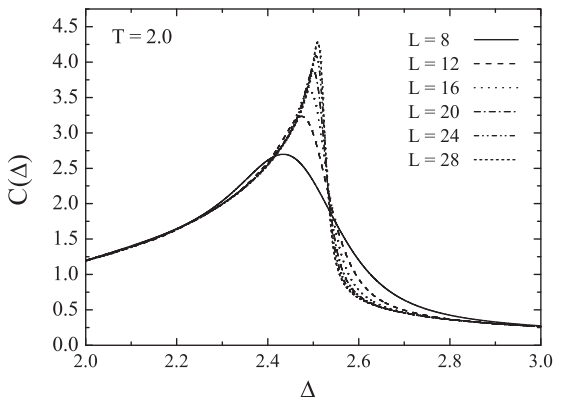

FIG. 3. Specific-heat curves as a function of the crystal field Δ for $T = 2.0$ and several system sizes in the second-order regime. Smooth curves typical of continuous transitions with a clear shift behavior are observed.

Similarly, we denote by C_L^* the value of the specific heat at this pseudocritical point $C(\Delta_L^*)$. The value of Δ_L^* is numerically determined by calculating the second derivative of $\langle E_J \rangle$ with respect to Δ, analogous to the above calculations, and finding the zero crossing. For this, we apply a bisection algorithm with time-series reweighting for the full data set, as well as w subsets, each excluding $1/w$ measurements, for the jackknife error calculation [34]. The jackknife method is similarly then used for C_L^*.

To sum up, using the above scheme, we have performed simulations for the three temperatures shown in Fig. 1 and outlined in the Introduction, as well as for the tricritical temperature $T_t = 1.4182$ [14]. In all cases, we considered various linear system sizes within the range $L = 8$–28. In principle, our numerical approach could as well simulate even larger system sizes, especially in the second-order regime. Still we have found it useful to optimize our code following the needs of a careful inspection of the first-order regime, for which linear sizes of the order of $L = 28$ are already quite large, taking into account that we are well into the low-temperature part of the phase diagram of the model.

III. FINITE-SIZE SCALING ANALYSIS

In this section, we present the main results of our contribution based on a FSS analysis of the numerical data obtained with the method outlined above. As a first step we consider the scaling in the second-order regime of the model ($T > T_t$) and, in particular, at the temperature $T_1 = 2.0$. Let us point out here that when it comes to the second-order transition regime of the BC model, the modified multicanonical method as implemented here is by no means the method of choice if one wants to obtain high-accuracy estimates of critical exponents (or critical points) and cannot compete against other cluster-update methods [35] or more involved generalized ensemble schemes [36,37] especially tailored to this situation. However, a qualitative study at this regime allows a direct comparison to the extensive and precise literature of the simple 3D Ising model, thus serving as a clear-cut test of the proposed scheme. Additionally, it justifies the results and conclusions drawn from our study in the first-order regime, presented later in this section for two temperature values ($T_2 = 1.0$ and $T_3 = 0.9$ in Fig. 1), which is not so easy to control given the huge energy barriers illustrated in Fig. 2(a). Finally, in the last part of this section, we discuss the scaling behavior of our observables at an estimate of the tricritical point [14].

Figure 3 displays the specific-heat-like curves defined in Eq. (7) as a function of the crystal field Δ for $T = 2.0$. Several system sizes up to $L = 28$ are shown which exhibit a clear shift behavior. This is further quantified in Fig. 4, which presents the FSS behavior of the pseudocritical fields Δ_L^* estimated as the locations where the specific heat attains its maximum. As usual, for second-order phase transitions a scaling behavior of the form

$$\Delta_L^* = \Delta_c + bL^{-1/\nu} \tag{8}$$

is used in order to describe the approach to the thermodynamic limit. It appears that this method of extracting pseudocritical points from the maxima of some properly defined thermodynamic quantity is capable of producing accurate estimates

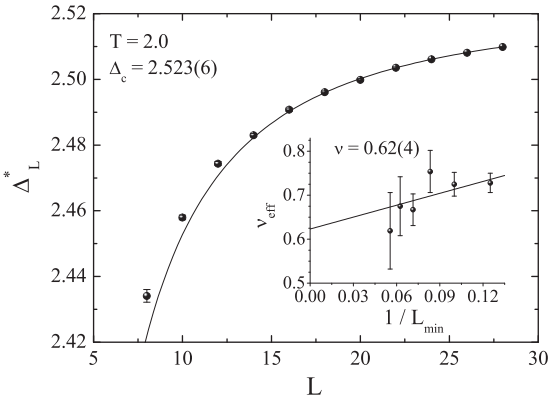

FIG. 4. Shift behavior (8) of the pseudocritical fields Δ_L^* at $T = 2.0$ obtained from the peak location of the specific-heat curves shown in Fig. 3. The solid line is a fit for linear sizes $L \geqslant L_{\min} = 18$, giving a stable, under $L_{\min}$ changes, critical field value $\Delta_c = 2.523(6)$. The inset illustrates the extrapolation of the effective exponent ν, obtained by varying the cutoff $L_{\min}$ of the fits, to the thermodynamic limit.

for both the critical crystal field Δ_c and the correlation-length exponent ν, assuming that its behavior follows the observed shift behavior of our pseudocritical fields Δ_L^*. It is well known from the general scaling theory that, even for simple models, the equality between the correlation-length exponent and the shift exponent is not a necessary consequence of scaling [38]. Of course, it is a general practice to assume that the correlation-length behavior can be deduced by the shift of appropriate thermodynamic functions.

In fact, the solid line in the main panel of Fig. 4 represents a fitting of the form (8), using as a lower cutoff the linear size $L_{\min} = 18$. We have performed this type of analysis for several values of $L_{\min}$ within the range 8–18 and keeping, of course, the upper system size fixed at $L_{\max} = 28$. For each of these fits we have estimated an effective value of the correlation-length exponent, which is plotted in the inset of Fig. 4 as a function of the inverse lower cutoff, i.e., the parameter $1/L_{\min}$. A linear extrapolation to the infinite-volume limit provides an estimate of $\nu = 0.62(4)$, which within error bars is compatible with the Ising universality exponent $\nu = 0.6304(13)$ [39], as expected. Regarding the value of the critical field, we obtain the estimate $\Delta_c(T_1 = 2.0) = 2.523(6)$, which remained quite stable under the switching of the lower cutoff during the fitting procedure. Thus, up to this point we have verified through a rather different, "orthogonal" route the expected Ising universality in the second-order phase transition regime of the 3D BC model.

We now move on to the main objective of this work, the discussion of the characteristics of the transition in the first-order regime and its dimensional scaling behavior. Let us point out here before discussing our findings that crossing the boundary at the first-order transition regime at a fixed temperature is an orthogonal approach to the fixed-field ansatz. One advantage in the case of the BC model is a broad temperature range with a first-order transition in comparison to a small Δ range.

As we discussed above, we have obtained numerical data at two temperatures in the first-order regime of the model, $T_2 = 1.0$ and $T_3 = 0.9$. A nice illustration of the first-order

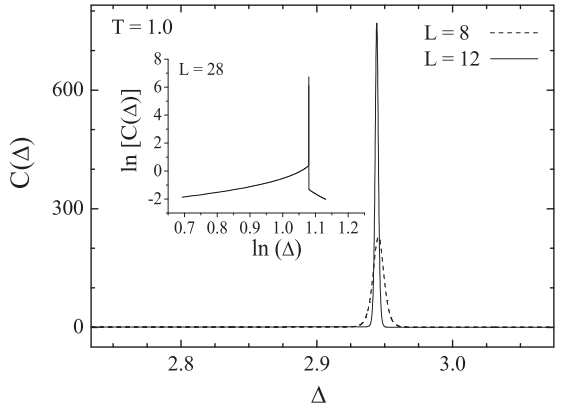

FIG. 5. Specific-heat curves as a function of the crystal field Δ at $T = 1.0$ and two system sizes $L = 8$ (dashed line) and 12 (solid line). The inset illustrates a typical first-order-like specific-heat curve for a system with linear size $L = 28$ on a double logarithmic scale.

character of the transition at these temperatures is shown in Fig. 5, where we plot the specific-heat curves obtained from Eq. (7) for $T = 1.0$ and two system sizes, $L = 8$ and $L = 12$ (and $L = 28$ in the inset on a double logarithmic scale). Clearly, a sharp peak is observed, which becomes much more pronounced with increasing system size.

Following a similar analysis as above, we study now the scaling of the pseudocritical fields Δ_L^* obtained from the sharp specific-heat peaks. In this case we would expect a scaling of the form

$$\Delta_L^* = \Delta^* + bL^{-d}, \tag{9}$$

where $d = 3$ is the dimensionality of the lattice and Δ^* the transition field. The above shift behavior of the pseudocritical fields Δ_L^* for both temperatures $T = 1.0$ and $T = 0.9$ in the first-order regime of the phase diagram is shown in Fig. 6 as a function of the inverse volume of the system. The solid lines are linear extrapolations to the infinite-volume limit (for a clearer

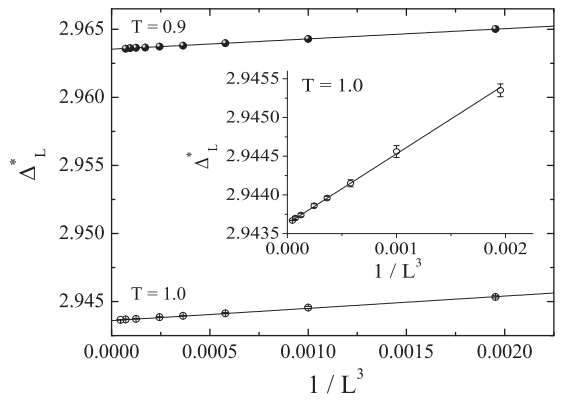

FIG. 6. Shift behavior (9) of the pseudocritical fields Δ_L^* obtained from the peak location of the specific-heat curves (a sample of which is shown in Fig. 5) for both temperatures $T = 1.0$ and $T = 0.9$ in the first-order regime of the phase diagram. The obtained transition fields Δ^* are given in the main text. The inset is a mere enlargement of the $\sim L^{-d}$ approach of the pseudotransition points Δ_L^* to $L \to \infty$ for the temperature $T = 1.0$.

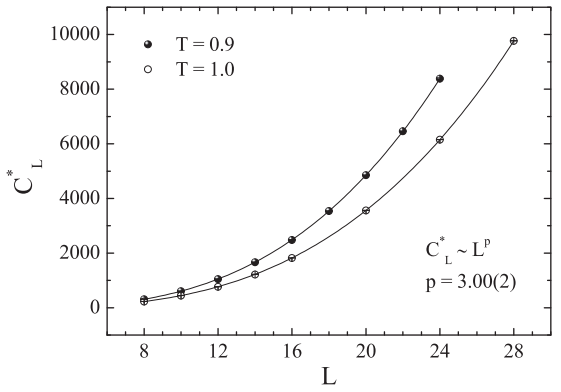

FIG. 7. Simultaneous fitting of the specific-heat maxima at both temperatures in the first-order regime. The expected $\sim L^d$ scaling behavior is obtained as can be clearly seen.

illustration of the linear behavior, see the corresponding inset). The obtained transition fields Δ^* are 2.944(5) and 2.964(6) for $T = 1.0$ and 0.9, respectively.

As another important aspect of the first-order regime in the phase diagram of the model, we study the scaling of the specific-heat maxima in Fig. 7. In particular, we plot the FSS behavior of the peaks for both temperatures considered in this regime, where the two solid lines show a simultaneous fitting attempt of the form $C_L^* \sim L^p$, meaning that the two data sets share the same exponent during the fitting procedure. Of course, in a standard first-order phase transition, the exponent p is expected to be equal to the dimensionality d of the system, which is 3 in our case. The result for the exponent p of a simultaneous fit to the data for both temperatures with $\chi^2/\mathrm{dof} \approx 0.8$ is $p = 3.00(2)$, which is in excellent agreement with the theoretical expectation $p = d = 3$.

Further, to the above successful study of criticality in the second-order regime of the model, it is now clear that the numerical method and scaling approach implemented in the present paper is able to capture as well the first-order characteristics of the transition within good accuracy. This latter fact is of particular importance as we are dealing with the low-temperature, first-order regime of the BC model, where it is common knowledge that most numerical methods fail to produce reliable estimates of transition points and criticality. Thus, the current method could be easily stretched to produce an accurate approximation of the phase boundary line for values of the crystal field Δ within the regime $[\Delta_t, 3]$.

The multicanonical method allows us to directly estimate the barrier associated with the suppression of states during the first-order phase transition, as shown in Fig. 2. Considering distributions with two peaks of equal height, i.e., two equally probably states, leads to the formulation of a free-energy-like barrier in the E_Δ space,

$$B = \frac{1}{2\beta\Delta} \ln\left(\frac{P_{\max}}{P_{\min}}\right)_{\mathrm{eqh}}, \tag{10}$$

where $P_{\max}$ and $P_{\min}$ are the maximum and the local minimum of the distribution $P(E_\Delta)$, respectively. The resulting barrier connects a spin-0 dominated regime (E_Δ small) and a spin-± 1 dominated regime (E_Δ large). This shows large similarities to the Ising (lattice gas) model and the according droplet-strip

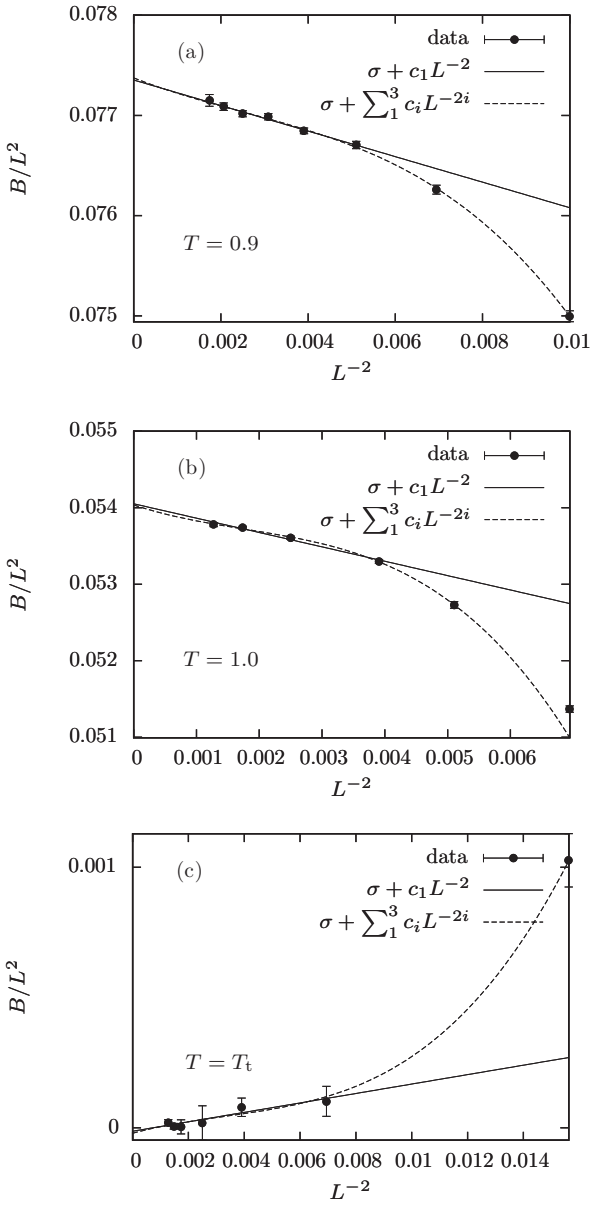

FIG. 8. Scaling of the barrier height B for all considered temperatures $T \leqslant T_t$. This barrier may be associated with the transition from a spin-0 dominated to a spin-± 1 dominated regime (see Fig. 2). Then B/L^2 plays the role of an interface tension for spin-0 strips.

transition [40,41]. Thus, the association with condensation and strip formation of spin-0 clusters seems natural and we would expect a scaling behavior in 3D as $B/L^2 = \sigma + c_1 L^{-2} + \mathcal{O}(L^{-4})$ possibly with higher-order corrections [42]. Figure 8 shows B/L^2 as a function of L^{-2} for $T_3 = 0.9$, $T_2 = 1.0$, and $T_t = 1.4182$ with fits of the data including the first correction and up to the third corrections. While higher-order corrections describe the systematic dependence of the data better, the $L \to \infty$ extrapolations are consistent within error bars for both fits, yielding the estimates $\sigma_3 = 0.0774(1)$ and $\sigma_2 = 0.0540(2)$ for $T_3 = 0.9$ and $T_2 = 1.0$, respectively. In the vicinity of the tricritical point, at $T_t = 1.4182$, the extrapolation yields $\sigma \approx 0$, indicating, as expected, that the interface tension vanishes in the thermodynamic limit.

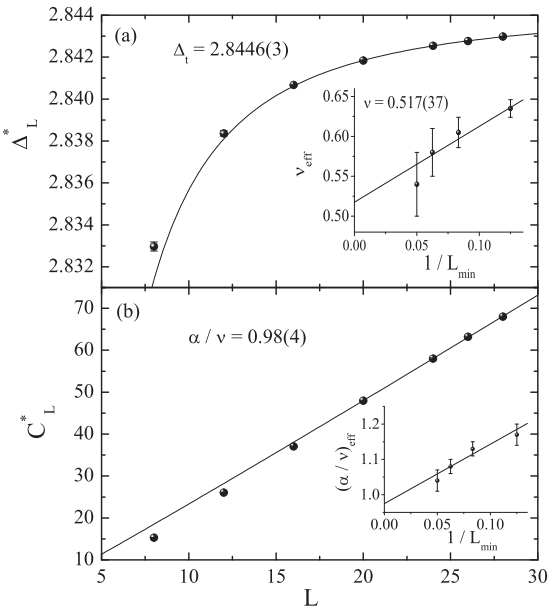

FIG. 9. Critical aspects of the 3D BC model at the tricritical point proposed in Ref. [14]: $T_t = 1.4182$. (a) Shift behavior of Δ_L^* obtained from the location of the specific-heat peaks. The solid line is a power-law fit of the form (8) for $L \geqslant L_{min} = 20$. The inset illustrates the infinite-volume extrapolation of the correlation-length effective exponent by varying the lower cutoff L_{min} of the fits. (b) Scaling behavior of the specific-heat peaks again for the larger system sizes. The corresponding inset shows an infinite-volume extrapolation of the effective exponent ratio α/ν using the same procedure as in (a).

In the last part of this section we discuss some scaling results in the vicinity of the tricritical point of the 3D BC model [3]. We have performed additional simulations by fixing the temperature at the tricritical estimate $T_t = 1.4182$, as suggested by Deserno [14], crossing again the phase diagram along the crystal-field axis. The results and relevant FSS analysis are given in Fig. 9, where one can clearly observe the departure from the Ising second-order universality class to the tricritical one, at least in terms of the estimated critical exponents. In particular, in panel (a) of this figure we present the shift behavior of Δ_L^* obtained from the location of the specific-heat peaks at the above defined temperature. The solid line is a power-law fitting of the form (8) for $L \geqslant L_{min} = 20$ and the estimate we obtain for the relevant (tricritical) crystal-field value is $\Delta_t = 2.8446(3)$. This latter value compares very well to the value 2.844 79(30) proposed by Deserno, using an empirical scaling of the coordinates of a latent-heat-like quantity of the model. The inset of panel (a) illustrates correspondingly the infinite-volume extrapolation of the correlation-length effective exponent by varying the cutoff L_{min} during the fitting procedure, as also performed in the analysis within the second-order regime of the model (see Fig. 4). The obtained value of $\nu = 0.517(37)$ is clearly different from that of the standard second-order Ising universality class and, within error bars, compatible to the theoretical expectation of the Ising tricritical universality value of $\nu = 0.5$ [3,16]. This result indicates that the estimate of

Deserno [14] for the location of the tricritical point in the temperature–crystal-field plane is indeed quite accurate, and, second, it provides a strong test in favor of the implemented numerical and scaling scheme of the present paper. Further, to these results, we present in Fig. 9(b) the scaling behavior of the specific-heat peaks C_L^*, following the scaling law $C_L^* \sim L^{\alpha/\nu}$. The solid line is a power-law fit of this form, again for the larger system sizes, and the corresponding inset illustrates the infinite-volume extrapolation of the effective exponent ratio α/ν. This analysis leads to an estimate $\alpha/\nu = 0.98(4)$, again very close to the expected Ising tricritical universality value of $\alpha/\nu = 1$ [3,16].

IV. CONCLUSIONS AND OUTLOOK

In this paper, we have presented a numerical study of the 3D BC model defined on a simple cubic lattice. By implementing a variant of the multicanonical method, we have performed simulations of the model keeping a constant temperature and crossing the phase boundary along the crystal-field axis. In this way we have obtained numerical data for several temperatures in both the first- and second-order regime of the model, as well as in the vicinity of the tricritical point. A standard FSS analysis, mainly based on a properly defined specific-heat-like quantity, provided us with precise estimates for the transition points in both regimes of the phase diagram and with a clear verification of the expected $\sim L^d$ scaling behavior and the Ising universality class in the first- and second-order regimes of the model, respectively.

An interesting feature of our study is related to the fact that we have been able to probe efficiently the low-temperature first-order regime of the phase diagram of the BC model, a rather tricky numerical task, and obtain accurate estimates of transition points in the regime of strong crystal fields. Using the multicanonical method, and hence simulating otherwise strongly suppressed states, allowed us to measure the associated free-energy-like barrier in the first-order regime up to the tricritical temperature. This barrier may be related to the interface tension for spin-0 droplets/strips, which we showed vanishes as one approaches the tricritical point from the first-order regime. Moreover, further numerical simulations performed at the tricritical temperature $T_t = 1.4182$, proposed by Deserno [14], indicated that this original estimate is rather accurate, verifying at the same time the expected Ising tricritical exponent values of $\nu = 0.5$ and $\alpha/\nu = 1$ from infinite-volume extrapolations of our effective exponents.

A further asset of the proposed numerical and scaling schemes is that it opens a new window for revisiting the effect of disorder in first-order phase transitions in both 2D and 3D, where a unified approach to universality is still missing. For instance, although it is known that in 2D under the presence of bond disorder the ex-second-order regime of the BC model falls into the universality class of the corresponding random Ising model along the lines of the strong universality hypothesis [18], the same is not true for the ex-first-order regime. Interestingly enough, for the ex-first-order regime different results have been obtained for different lattice geometries [18,20]. The situation in 3D is even more ambiguous, where one has to be also careful with respect to the diffused amount of disorder in the system in order to secure the switching to a continuous transition [43,44]. A recent study of the random version of the 3D BC model suggested a possible new universality class at the ex-first-order regime, different from that at the ex-second-order regime [19], an interesting finding if one considers that the two transitions are between the same ferromagnetic and paramagnetic phases. Yet, the authors of Ref. [19] clearly underlined the need for a more sophisticated approach (in both numerical and scaling terms) in order to tackle efficiently the low-temperature disorder-induced continuous transition regime of the model.

To conclude, using as a platform the BC model that shows the unique feature of having continuous and first-order transition lines in its phase diagram, we believe that the practice followed in the present paper applied over a wide range of disorder-strength values and temperatures will provide a better understanding of the effect of disorder in spin systems. Using the parallelized version of the multicanonical method and crossing the phase boundary along the crystal-field axis, we expect to be able to study systematically the universality class and scaling corrections at the disorder-induced, second-order phase transition of the BC model, the shift behavior of the tricritical point as a function of the disorder strength, and other relevant open questions. Research in this direction is currently under way.

ACKNOWLEDGMENTS

This project was funded by the European Union and the Free State of Saxony. Part of this work has been financially supported by the Leipzig Graduate School of Excellence GSC185 "BuildMoNa", the Deutsch-Französische Hochschule DFH-UFA (Grant No. CDFA-02-07), and the EU IRSES Network DIONICOS (Grant No. 612 707).

[1] M. Blume, Phys. Rev. **141**, 517 (1966).
[2] H. W. Capel, Physica (Utrecht) **32**, 966 (1966); **33**, 295 (1967); **37**, 423 (1967).
[3] I. D. Lawrie and S. Sarbach, in *Phase Transitions and Critical Phenomena*, edited by C. Domb and J. L. Lebowitz (Academic Press, London, 1984), Vol. 9, pp. 1–161.
[4] W. Selke and J. Oitmaa, J. Phys. C: Condens. Matter **22**, 076004 (2010).
[5] N. S. Branco and B. M. Boechat, Phys. Rev. B **56**, 11673 (1997).
[6] D. P. Landau, Phys. Rev. Lett. **28**, 449 (1972); A. N. Berker and M. Wortis, Phys. Rev. B **14**, 4946 (1976); M. Kaufman, R. B. Griffiths, J. M. Yeomans, and M. E. Fisher, *ibid.* **23**, 3448 (1981); W. Selke and J. Yeomans, J. Phys. A: Math. and Gen. **16**, 2789 (1983); D. P. Landau and R. H. Swendsen, Phys. Rev. B **33**, 7700 (1986); J. C. Xavier, F. C. Alcaraz, D. Penã Lara, and J. A. Plascak, *ibid.* **57**, 11575 (1998).

[7] M. J. Stephen and J. L. McCauley Jr., Phys. Lett. **44A**, 89 (1973); T. S. Chang, G. F. Tuthill, and H. E. Stanley, Phys. Rev. B **9**, 4882 (1974); G. F. Tuthill, J. F. Nicoll, and H. E. Stanley, *ibid.* **11**, 4579 (1975); F. J. Wegner, Phys. Lett. **54A**, 1 (1975).

[8] P. F. Fox and A. J. Guttmann, J. Phys. C **6**, 913 (1973); T. W. Burkhardt and R. H. Swendsen, Phys. Rev. B **13**, 3071 (1976); W. J. Camp and J. P. Van Dyke, *ibid.* **11**, 2579 (1975); D. M. Saul, M. Wortis, and D. Stauffer, *ibid.* **9**, 4964 (1974).

[9] P. Nightingale, J. Appl. Phys. **53**, 7927 (1982).

[10] P. D. Beale, Phys. Rev. B **33**, 1717 (1986).

[11] A. K. Jain and D. P. Landau, Phys. Rev. B **22**, 445 (1980).

[12] D. P. Landau and R. H. Swendsen, Phys. Rev. Lett. **46**, 1437 (1981).

[13] C. M. Care, J. Phys. A: Math. Gen. **26**, 1481 (1993).

[14] M. Deserno, Phys. Rev. E **56**, 5204 (1997).

[15] H. W. J. Blöte, E. Luijten, and J. R. Heringa, J. Phys. A: Math. Gen. **28**, 6289 (1995).

[16] Y. Deng and H. W. J. Blöte, Phys. Rev. E **70**, 046111 (2004).

[17] C. J. Silva, A. A. Caparica, and J. A. Plascak, Phys. Rev. E **73**, 036702 (2006).

[18] A. Malakis, A. N. Berker, I. A. Hadjiagapiou, and N. G. Fytas, Phys. Rev. E **79**, 011125 (2009); A. Malakis, A. N. Berker, I. A. Hadjiagapiou, N. G. Fytas, and T. Papakonstantinou, *ibid.* **81**, 041113 (2010).

[19] A. Malakis, A. N. Berker, N. G. Fytas, and T. Papakonstantinou, Phys. Rev. E **85**, 061106 (2012).

[20] P. E. Theodorakis and N. G. Fytas, Phys. Rev. E **86**, 011140 (2012).

[21] N. G. Fytas, Eur. Phys. J. B **79**, 21 (2011).

[22] N. G. Fytas and P. E. Theodorakis, Eur. Phys. J. B **86**, 30 (2013).

[23] B. A. Berg and T. Neuhaus, Phys. Lett. B **267**, 249 (1991); Phys. Rev. Lett. **68**, 9 (1992).

[24] W. Janke, Int. J. Mod. Phys. C **03**, 1137 (1992); Phys. A (Amsterdam, Neth.) **254**, 164 (1998).

[25] J. Zierenberg, M. Marenz, and W. Janke, Comput. Phys. Commun. **184**, 1155 (2013); Phys. Procedia **53**, 55 (2014).

[26] W. Janke, in *Computational Many-Particle Physics*, edited by H. Fehske, R. Schneider, and A. Weiße, Lecture Notes in Physics Vol. 739 (Springer, Berlin, 2008), pp. 79–140.

[27] F. Wang and D. P. Landau, Phys. Rev. Lett. **86**, 2050 (2001); Phys. Rev. E **64**, 056101 (2001).

[28] M. Troyer, S. Wessel, and F. Alet, Phys. Rev. Lett. **90**, 120201 (2003).

[29] P. Dayal, S. Trebst, S. Wessel, D. Würtz, M. Troyer, S. Sabhapandit, and S. N. Coppersmith, Phys. Rev. Lett. **92**, 097201 (2004).

[30] R. E. Belardinelli and V. D. Pereyra, Phys. Rev. E **75**, 046701 (2007).

[31] N. G. Fytas, A. Malakis, and K. Eftaxias, J. Stat. Mech. (2008) P03015.

[32] S. Schöbl, J. Zierenberg, and W. Janke, Phys. Rev. E **84**, 051805 (2011).

[33] A. K. Hartmann and A. P. Young, Phys. Rev. B **64**, 180404 (2001).

[34] B. Efron, *The Jackknife, the Bootstrap and other Resampling Plans* (Society for Industrial and Applied Mathematics, Philadelphia, 1982).

[35] M. Hasenbusch, Phys. Rev. B **82**, 174434 (2010).

[36] B. A. Berg and W. Janke, Phys. Rev. Lett. **98**, 040602 (2007); Phys. Procedia **7**, 19 (2010).

[37] E. Bittner and W. Janke, Phys. Rev. E **84**, 036701 (2011).

[38] M. N. Barber, in *Phase Transitions and Critical Phenomena*, edited by C. Domb and J. L. Lebowitz (Academic Press, New York, 1983), Vol. 8, pp. 145–266.

[39] R. Guida and J. Zinn-Justin, J. Phys. A: Math. Gen. **31**, 8103 (1998).

[40] A. Nußbaumer, E. Bittner, T. Neuhaus, and W. Janke, Europhys. Lett. **75**, 716 (2006).

[41] A. Nußbaumer, E. Bittner, and W. Janke, Phys. Rev. E **77**, 041109 (2008).

[42] E. Bittner, A. Nußbaumer, and W. Janke, Nucl. Phys. B **820**, 694 (2009).

[43] K. Hui and A. N. Berker, Phys. Rev. Lett. **62**, 2507 (1989); **63**, 2433(E) (1989).

[44] A. N. Berker, Phys. A (Amsterdam, Neth.) **194**, 72 (1993).